JOURNAL OF SOLID STATE CHEMISTRY 58, 204–210 (1985)

Structure and Luminescence of the α-$Ln$$Nb_3O_9$-Type Rare Earth Niobates

C. C. TORARDI, L. H. BRIXNER, AND C. M. FORIS

Central Research and Development Department,[1] *E. I. du Pont de Nemours and Company, Experimental Station, Wilmington, Delaware 19898*

Received September 17, 1984; in revised form November 28, 1984

α-$Ln$$Nb_3O_9$ (Ln = La, Pr, Nd) compounds have been prepared hydrothermally from acidic solutions. In comparison to the previously reported orthorhombic β modifications, α-$Ln$$Nb_3O_9$ compounds are monoclinic. The structure of α-$PrNb_3O_9$ was determined with a = 5.3784(6), b = 7.602(2), c = 16.344(2) Å, and β = 92.21(1)°, space group $P2_1/c$. It is built of double and single chains of corner-shared NbO_6 octahedra extended along the b axis. Praseodymium atoms reside in tunnels along the b axis and are in eight-coordination with oxygen. All α-$Ln$$Nb_3O_9$ compounds can be irreversibly converted to the β modification by heating in air to 1200°C. The X-ray excited luminescence of Sm-, Eu-, Tb-, and Dy-doped α-$LaNb_3O_9$ is also reported.

Introduction

$Ln$$Nb_3O_9$ compounds (where Ln = La, Ce, Pr, and Nd) were first reported by Iyer and Smith (*1*) and described as orthorhombically distorted perovskites with rare earth cation vacancies. These compounds were prepared between 1360 and 1400°C and we shall henceforth refer to them as the β or high-temperature modification.

We have recently described (*2*) a new rare earth haloniobate of the formula $LaNb_2O_6Cl$, which was obtained by the interaction of LaOCl and Nb_2O_5 in a sealed tube. Efforts to prepare the corresponding $PrNb_2O_6Cl$ at 900°C by the same technique failed and yielded the new compound $Pr_3NbO_4Cl_6$ (*3*). As a by-product, we also obtained plate-like green crystals of α-$PrNb_3O_9$, which is isostructural with the low-temperature form of $LaNb_3O_9$ reported by Sturm and Gruehn (*4*). This rather uncontrolled technique prompted us to search for a more reliable and reproducible way to prepare the low temperature modifications of these niobates. The present paper describes the hydrothermal preparation of α-$Ln$$Nb_3O_9$ compounds where Ln = La, Pr, and Nd with the latter two being new materials. The structure and subcell of α-$PrNb_3O_9$ are discussed, and the synthesis and luminescence of Sm, Eu-, Tb-, and Dy-doped α-$LaNb_3O_9$ are also described.

Experimental

Synthesis

α-$Ln$$Nb_3O_9$ (Ln = La, Pr, Nd) compounds were prepared hydrothermally in an acidic chloride solution. A 1 : 1 : 30 mole ratio of Nb_2O_5 (Kawecki, optical grade), LnOCl, and distilled H_2O was sealed in a

[1] Contribution No. 3600.

0022-4596/85 $3.00

gold tube, held at 700°C and 3 kbar pressure for 16 hr, slowly cooled at 25°/hr to 400°C, and then quenched. Attempts to synthesize the Sm and Gd compounds by this technique were unsuccessful. Rare-earth-doped compounds α-La$_{0.94}Ln_{0.06}$Nb$_3$O$_9$ (Ln = Sm, Eu, Tb, and Dy) were synthesized starting with La$_{0.94}Ln_{0.06}$OCl compounds which were prepared as previously described (*5*). Long, rectangular plate- and rod-shaped crystals up to 1 mm in the largest dimension were obtained routinely. The undoped lanthanum compound was also prepared by reacting stoichiometric quantities of La$_2$O$_3$ and Nb$_2$O$_5$ in 2 *M* HCl solution under the same conditions described above. All α-LnNb$_3$O$_9$ preparations showed a small amount of LnNbO$_4$ in their respective X-ray powder diffraction patterns.

β-LnNb$_3$O$_9$ compounds were prepared from the α-LnNb$_3$O$_9$ phases by heating them in air at 1200–1250°C for 1–3 days in high-purity (99.8%) recrystallized alumina boats. A small quantity of LnNb$_5$O$_{14}$ was observed in the X-ray powder diffraction patterns. This impurity may arise from reaction with the alumina boat, forming LnAlO$_3$ as the other by-product.

X-Ray Powder Diffraction

X-Ray powder diffraction patterns were obtained with a Guinier–Hägg-type focusing camera (r = 40 mm) equipped with a quartz monochromator. The radiation was Cu$K\alpha_1$ (λ = 1.5405 Å) and the internal standard was Si (a = 5.4305 Å). An Optronics P-1700 Photomation instrument was used to collect absorbance data from the films. Peak positions and relative intensities were determined with local computer programs. The lattice parameters were refined by a least-squares procedure.

X-Ray powder diffraction data for monoclinic α-PrNb$_3$O$_9$ and orthorhombic β-PrNb$_3$O$_9$ are given in Tables I and II, respectively. Lattice parameters for the α and β forms of LnNb$_3$O$_9$ (Ln = La, Pr, and Nd) are given in Table III. For each of the three α modifications, only one or two weak lines could be uniquely indexed with *hkl*: $l \neq 2n$. The presence of a subcell with $c/2$ was investigated using single crystal X-ray diffraction data (see below).

TABLE I

X-RAY POWDER DIFFRACTION DATA FOR MONOCLINIC α-PrNb$_3$O$_9$[a]

2θ(obs)	I(obs)	*hkl*	d(obs)	d(calc)
10.803	50	002	8.182	8.170
15.885	16	012	5.574	5.569
20.105	15	102	4.413	4.413
21.716	4	004	4.089	4.085
22.653	22	−112	3.922	3.919
23.358	49	020	3.805	3.806
23.974	2	021	3.709	3.707
24.717	20	014	3.599	3.599
25.798	50	022	3.450	3.450
26.873	100	−104	3.315	3.314
27.908	91	104	3.194	3.194
28.722	73	120	3.105	3.106
30.323	8	114	2.945	2.945
30.547	48	−122	2.924	2.925
31.013	80	122	2.881	2.882
32.124	30	024	2.784	2.785
33.313	60	200	2.687	2.687
34.957	12	016	2.565	2.564
35.536	5	202	2.524	2.524
35.893	18	−124	2.500	2.499
36.779	11	−212	2.442	2.445
37.069	8	032	2.423	2.423
37.568	23	106	2.392	2.392
38.320	8	−116	2.347	2.347
39.223	16	130	2.295	2.294
39.460	19	116	2.282	2.282
40.714	22	026	2.214	2.215
40.845	3	204	2.207	2.207
41.064	4	220	2.196	2.195
41.212	20	−214	2.189	2.189
41.873	8	034	2.156	2.155
42.258	13	−222	2.137	2.137
42.972	17	222	2.103	2.104
44.305	9	008	2.043	2.042
44.951	8	−134	2.015	2.015
46.303	17	−224	1.959	1.959
47.567	10	224	1.910	1.909

[a] F_{20} = 59(0.008, 42) (*6*); M_{20} = 39 (*7*).

TABLE II

X-RAY POWDER DIFFRACTION DATA FOR ORTHORHOMBIC β-$PrNb_3O_9$[a]

2θ(obs)	I(obs)	hkl	d(obs)	d(calc)
11.258	89	001	7.853	7.850
22.647	88	002	3.923	3.925
22.657	80	010	3.921	3.913
22.844	77	100	3.889	3.889
25.430	72	011	3.500	3.502
25.525	66	101	3.487	3.485
32.295	99	012	2.770	2.771
32.448	100	110	2.757	2.758
34.219	20	003	2.618	2.617
34.433	32	111	2.602	2.602
41.516	9	013	2.173	2.175
46.206	73	004	1.963	1.963
46.380	84	020	1.956	1.956
46.679	79	200	1.944	1.944
47.860	49	113	1.899	1.898
48.175	10	201	1.887	1.887
52.150	25	104	1.752	1.752
52.279	13	120	1.748	1.748
52.481	27	202	1.742	1.742
53.690	18	121	1.706	1.706
53.876	18	211	1.700	1.700
57.598	75	114	1.599	1.599
57.698	78	122	1.596	1.597
57.880	75	212	1.592	1.592
58.879	8	023	1.567	1.567
59.140	9	203	1.561	1.561
63.825	20	015	1.457	1.457
67.549	36	024	1.386	1.386
67.808	41	204	1.381	1.381
67.908	46	220	1.379	1.379
72.328	11	124	1.305	1.305
72.571	12	222	1.302	1.301

[a] F_{20} = 60(0.014, 23) (6); M_{20} = 61 (7).

TABLE III

LATTICE PARAMETERS OF THE MONOCLINIC (α) AND ORTHORHOMBIC (β) $Ln$$Nb_3O_9$ COMPOUNDS

Ln	a (Å)	b (Å)	c (Å)	β (deg)	V (Å^3)
La	5.441(1)	7.669(1)	16.331(3)	92.19(2)	680.9(1)
Pr	5.379(1)	7.612(1)	16.352(2)	92.19(1)	668.9(1)
Nd	5.354(1)	7.595(1)	16.357(2)	92.28(1)	664.6(1)
La	3.9175(3)	3.9142(3)	7.9120(6)		121.32(2)
Pr	3.8890(4)	3.9128(4)	7.8504(8)		119.46(2)
Nd	3.8818(7)	3.9083(6)	7.834(1)		118.86(2)

Single Crystal X-Ray Structure Determination

A long, columnar-shaped crystal of α-$PrNb_3O_9$ with dimensions 0.034 × 0.030 × 0.280 mm was placed on an Enraf–Nonius CAD4 X-ray diffractometer equipped with a graphite monochromator and MoK_α radiation. From settings of 25 reflections, the lattice parameters of the monoclinic cell were refined to a = 5.3784(6), b = 7.602(2), c = 16.344(2) Å, and β = 92.21(1)°. For Z = 4, the calculated density is 5.61 g · cm^{-3}.

A total of 2230 reflections were collected by the ω mode from $2 \leq \theta \leq 30°$ and merged to yield 1615 independent data with $I \geq 2\sigma(I)$ in $2/m$ symmetry. The data were treated for Lorentz and polarization effects, and an analytical correction for absorption was applied (μ = 119.8 cm^{-1}).

An examination of the data revealed systematic absences compatible with space group $P2_1/c$ (No. 14). The structure was determined using the heavy atom method. Full-matrix least-squares refinement on all positional and anisotropic thermal parameters including terms for anomalous dispersion for La and Nb and for anisotropic extinction converged with R = 0.025 and R_w = 0.032. The largest peak in a final difference Fourier was 0.75 e/Å^3 near the Pr atom.[2]

Results and Discussion

Structure Description

Atomic positional and thermal parameters for α-$PrNb_3O_9$ are listed in Table IV and important interatomic distances are given in Table V.

The details of the α-$PrNb_3O_9$ structure are essentially identical to those of the pre-

[2] All crystallographic calculations were performed on a Digital Equipment Corp. VAX 11/780 computer using a system of programs developed by J. C. Calabrese. Structural plots were made with the assistance of the ORTEP program (C. K. Johnson, 1976).

TABLE IV

POSITIONAL[a] AND THERMAL[b] PARAMETERS FOR THE ATOMS OF α-$PrNb_3O_9$

Atom	x	y	z	B_{11}	B_{22}	B_{33}	B_{12}	B_{13}	B_{23}
Pr	0.96739(5)	0.24992(4)	0.03144(2)	0.43(1)	0.39(1)	0.54(1)	0.00(1)	0.07(1)	0.00(1)
Nb1	0.00839(13)	0.53038(6)	0.24854(5)	0.52(2)	0.42(2)	0.33(2)	−0.04(2)	0.12(1)	0.03(2)
Nb2	0.52221(12)	0.00055(6)	0.39952(5)	0.43(2)	0.37(2)	0.31(2)	0.01(1)	0.05(2)	0.02(1)
Nb3	0.47274(12)	0.51472(7)	0.60007(4)	0.42(2)	0.49(2)	0.29(2)	−0.03(1)	0.07(2)	0.00(1)
O1	0.3201(7)	0.0545(6)	0.3103(2)	0.8(1)	0.8(2)	0.6(1)	0.0(1)	0.0(1)	0.0(1)
O2	0.1518(7)	0.0538(6)	0.6437(2)	0.6(1)	0.6(2)	0.4(1)	0.1(1)	0.1(1)	0.1(1)
O3	0.0966(7)	0.7542(6)	0.2409(3)	0.9(1)	0.5(1)	0.9(1)	−0.1(1)	0.3(1)	−0.1(1)
O4	0.6835(7)	0.9509(6)	0.1890(3)	0.6(1)	0.7(1)	0.8(2)	−0.1(1)	0.0(1)	0.1(1)
O5	0.1544(7)	0.0599(6)	0.1437(2)	0.6(1)	0.8(2)	0.4(1)	0.1(1)	0.1(1)	0.1(1)
O6	0.2652(7)	0.0357(6)	0.9835(3)	0.6(1)	0.6(1)	0.3(1)	−0.1(1)	0.2(1)	−0.2(1)
O7	0.2649(7)	0.0365(6)	0.4833(3)	0.4(1)	0.7(1)	0.4(1)	0.1(1)	0.0(1)	0.0(1)
O8	0.3548(7)	0.7491(5)	0.0814(2)	0.7(1)	0.4(1)	0.6(1)	−0.1(1)	−0.1(1)	−0.1(1)
O9	0.5595(7)	0.2501(5)	0.0954(2)	0.7(1)	0.3(1)	0.7(1)	−0.1(1)	0.2(1)	0.1(1)

[a] Space group $P2_1/c$ (No. 14).
[b] $\exp[-0.25(B_{11}h^2a^{*2} \ldots + 2(B_{12}hka^*b^* \ldots))]$.

viously reported low-temperature form of $LaNb_3O_9$ (*4*). α-$PrNb_3O_9$ contains double chains of distorted NbO_6 octahedra which share opposite corners along the chain in the *b* direction, and share edges across the chain. Figure 1 shows a section of the unit cell viewed along the *b* axis. Across the shared edge, the Nb–Nb distance is 3.30 Å.

TABLE V

IMPORTANT INTERATOMIC DISTANCES (Å) IN α-$PrNb_3O_9$

Pr–O2	2.537(4)	Nb1–O1	1.987(4)
Pr–O5	2.514(4)	Nb1–O2	2.011(4)
Pr–O6	2.434(4)	Nb1–O3	2.182(4)
Pr–O6′	2.513(4)	Nb1–O3′	1.772(4)
Pr–O7	2.432(4)	Nb1–O4	2.006(4)
Pr–O7′	2.518(5)	Nb1–O5	2.010(4)
Pr–O8	2.482(4)		
Pr–O9	2.466(4)		
Nb2–O1	1.832(4)	Nb3–O4	1.827(4)
Nb2–O2	1.959(4)	Nb3–O5	1.964(4)
Nb2–O7	2.211(5)	Nb3–O6	2.204(5)
Nb2–O7′	2.003(4)	Nb3–O6′	2.007(4)
Nb2–O8	2.022(4)	Nb3–O8	1.924(4)
Nb2–O9	1.956(4)	Nb3–O9	2.069(4)
Nb2–Nb2	3.302(1)	Nb3–Nb3	3.303(2)

Within the double chains, the Nb–O bond lengths average 2.00 Å for both Nb2 and Nb3 which agrees quite well with the sum of ionic radii (*8*). Double chains are interconnected by single chains of corner-sharing NbO_6 octahedra which are also parallel with the *b* axis. The six Nb1–O bond lengths in these chains also have an average value of 2.00 Å and include one short distance of 1.772 Å. This environment is similar to the niobium coordination in $NbOPO_4$ (*9*). Along both types of chains, the octahedra are alternately tipped forming a zig-zag

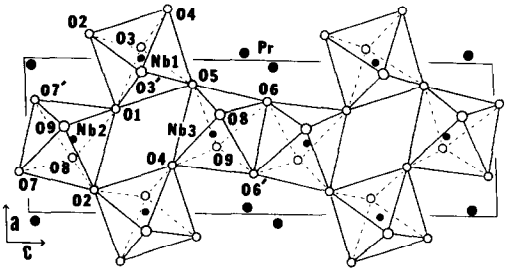

FIG. 1. A view along the *b* axis of α-$PrNb_3O_9$ showing the connected NbO_6 octahedra, and the tunnels in which the Pr atoms are located.

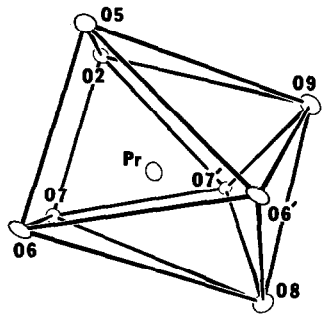

FIG. 2. An ORTEP drawing showing the coordination around praseodymium in α-$PrNb_3O_9$.

pattern in the *ab* plane. This gives rise to bent bond angles for Nb1–O3–Nb1, Nb2–O8–Nb3, and Nb2–O9–Nb3 of 147.9(2)°, 138.0(2)°, and 153.4(2)°, respectively.

Tunnels running in the *b* direction are created by the framework of NbO_6 octahedra. Praseodymium atoms are located in these tunnels at levels in between the niobium atoms (Fig. 1). Eight oxygen atoms are bonded to praseodymium in a bicapped trigonal-prismatic arrangement (Fig. 2) with Pr–O bond distances ranging from 2.432 to 2.537 Å. Four of these oxygen atoms (O6, O6′, O7, O7′) are each bonded to another Pr atom and two Nb atoms while the remaining four are shared with only two Nb atoms. The average Pr–O bond length of 2.487 Å compares well with the sum of ionic radii (2.50 Å) (*8*). Structurally, α-$PrNb_3O_9$ is related to $CaTa_2O_6$ (*10*) where only double chains of TaO_6 octahedra are present. All NbO_6 octahedra and LnO_8 polyhedra in these α-$LnNb_3O_9$ compounds have C_1 point group symmetry.

It was evident from axial oscillation photographs that a dominant subcell with $c/2$ was present in α-$PrNb_3O_9$. In order to determine the reason for the doubled c axis, an analysis of the subcell structure was also made. After eliminating all reflections with hkl: $l \neq 2n$ and dividing all remaining l indices by 2, a very good least-squares anisotropic structural refinement was obtained using 990 reflections in space group $P2_1/m$ ($R = 0.019$, $R_w = 0.030$). In the subcell, one of the niobium atoms (Nb1 of the true cell) was disordered within its octahedron with a Nb–Nb site separation along the y axis of 0.48 Å. These sites, which are each 50% occupied by niobium, are related by a center of symmetry. All other atomic positions and temperature factors were normal.[3] The real c axis is apparently due to an ordered positioning of these Nb atoms. This accounts for the approximate relation of x, y, $\frac{1}{2} + z$ in the atomic positional coordinates of Table IV.

A slow reconstructive phase transformation to the orthorhombic β form occurs at temperatures between 1050 and 1150°C for α-$LnNb_3O_9$ compounds. In the case of $PrNb_3O_9$, this structural change is accompanied by a 7.1% increase in normalized cell volume and a decrease in calculated density from 5.60 to 5.22 g · cm^{-3} which is consistent with a high-temperature modification. Heating the β form below the transformation temperature leaves this phase unchanged.

It is interesting to note that the very different α- and β-$LnNb_3O_9$ structures exist only up to neodymium. In contrast, all of the rare earths including yttrium can be incorporated into the perovskite-related $LnTa_3O_9$ structure which is isostructural with the β-$LnNb_3O_9$ modification (*1*). This observation suggests that the size of the rare earth ion may not be as important a feature as possible electronic differences in the Nb^{5+} and Ta^{5+} ions. Our attempts to prepare a low-temperature form of the $LnTa_3O_9$ compounds have been unsuccessful.

Luminescence

α-$LaNb_3O_9$ has also been used as a host for the fluorescing rare earths Ln = Sm, Eu, Tb, and Dy at a concentration of x =

[3] Atomic positional and thermal parameters for the α-$PrNb_3O_9$ subcell are available from the authors.

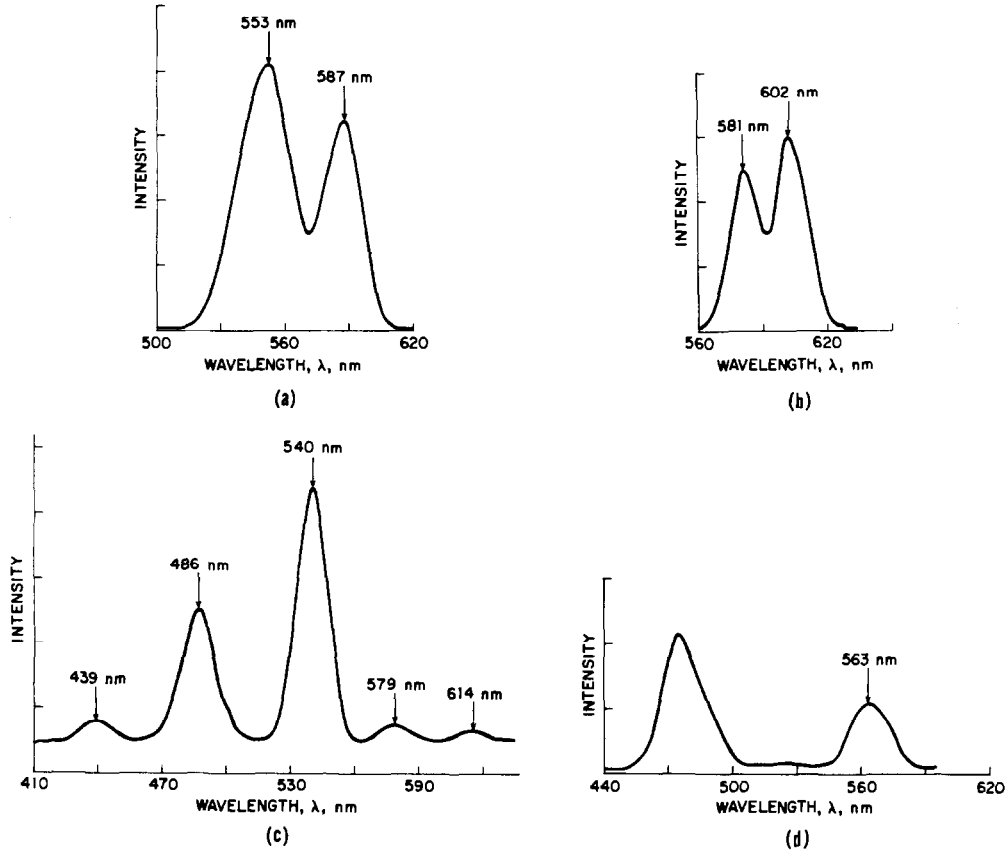

FIG. 3. 30-kVp (Mo radiation) X-ray excited fluorescent emission spectra of α-$La_{0.94}Ln_{0.06}Nb_3O_9$. Ln = Sm(a), Eu(b), Tb(c), and Dy(d).

0.06 in $La_{1-x}Ln_xNb_3O_9$ which is close to the optimum activator concentration.

These compounds were excited with 30 kVp Mo radiation in an experimental set up described recently (*11*). The fluorescent emission spectra are shown in Fig. 3. The relatively broad emission lines are not indicative of a poor state of crystallinity of the compositions but are rather due to the broad slitwidth employed. The emission of both the Sm- and Dy-doped samples was significantly weaker than that of the Eu- and Tb-doped materials. In the Eu case, the strength of the normally forbidden spin ($J = 0 \rightarrow J = 0$) $^5D_0 \rightarrow {}^7F_0$ line at 581 nm is surprising. Since the location of the other (602 nm) line is close to the center of the magnetic dipole transition $^5D_0 \rightarrow {}^7F_1$ and the electric dipole transition $^5D_0 \rightarrow {}^7F_2$, it could be that the individual lines are not resolved. In the Tb case the high-energy $^5D_3 \rightarrow {}^7F_j$ manifold is weaker than the $^5D_4 \rightarrow {}^7F_j$ lines. This is most likely the result of the relatively high Tb concentration in the sample.

It became obvious that for more detailed luminescent studies, and particularly for the correlation between structure and luminescence, UV-excited spectra at low temperature as well as fluorescence lifetime measurements would be necessary. We, therefore, entered into a joint study with the University of Utrecht, and these results will be published in the very near future.

References

1. P. N. Iyer and A. J. Smith, *Acta Crystallogr.* **23,** 740 (1967).
2. J. C. Calabrese, L. H. Brixner, and C. M. Foris, *J. Solid State Chem.* **48,** 142 (1983).
3. L. H. Brixner, J. C. Calabrese, and C. M. Foris, *Mater. Res. Bull.* **18,** 1493 (1983).
4. J. Sturm and R. Gruehn, *Naturwissenschaften* **62,** 296 (1975).
5. L. H. Brixner, J. F. Ackerman, and C. M. Foris, *J. Lumin.* **26,** 1 (1981).
6. G. S. Smith and R. L. Snyder, *J. Appl. Crystallogr.* **12,** 60 (1979).
7. P. M. de Wolff, *J. Appl. Crystallogr.* **1,** 108 (1968).
8. R. D. Shannon, *Acta Crystallogr. Sect. A* **32,** 751 (1976).
9. J. M. Longo and P. Kierkegaard, *Acta Chem. Scand.* **20,** 72 (1966).
10. L. Jahnberg, *Acta Chem. Scand.* **71,** 2548 (1963).
11. L. H. Brixner and H.-Y. Chen, *J. Electrochem. Soc.* **130,** 2435 (1983).